

The atomic and electronic structure of the $\{211\}/\{111\}$ facets in Si

This article has been downloaded from IOPscience. Please scroll down to see the full text article.

1989 J. Phys.: Condens. Matter 1 8251

(<http://iopscience.iop.org/0953-8984/1/43/025>)

View [the table of contents for this issue](#), or go to the [journal homepage](#) for more

Download details:

IP Address: 171.66.16.96

The article was downloaded on 10/05/2010 at 20:44

Please note that [terms and conditions apply](#).

LETTER TO THE EDITOR

The atomic and electronic structure of the $\{211\}/\{111\}$ facets in Si

M Kohyama[†], S Kose[†], M Kinoshita[†] and R Yamamoto[‡]

[†] Glass and Ceramic Material Department, Government Industrial Research Institute (MITI), Osaka, 1-8-31, Midorigaoka, Ikeda, Osaka 563, Japan

[‡] Department of Metallurgy and Materials Science, Faculty of Engineering, University of Tokyo, Bunkyo-ku, Tokyo 113, Japan

Received 30 June 1989, in final form 14 August 1989

Abstract. The atomic and electronic structure of the $\{211\}/\{111\}$ facets in Si have been examined based on the atomic model of Bourret and Bacmann. The optimum atomic structure has been determined by energy-minimisation calculations in the Keating model, and the electronic structure has been calculated using a supercell technique and a tight-binding model. Relatively large distortions exist at one of the two types of facet junctions between the $\{211\}$ and $\{111\}$ interfaces. This distorted region considerably influences the electronic structure at the facet junction compared with that at the other regions. However, there are no states introduced inside the minimum gap.

It is important to confirm the origins of the observed activity of grain boundaries in polycrystalline semiconductors. From various experiments [1–5], observations [6, 7] and theoretical calculations [8–13], it can be considered that the frequently observed coincident-site-lattice (CSL) boundaries such as the $\{111\}\Sigma = 3$, $\{211\}\Sigma = 3$ and $\{221\}\Sigma = 9$ boundaries in Si or Ge are electrically non-active because of atomic reconstruction at the interfaces. In our previous works [12, 13], we have shown by theoretical calculations that there are no deep states in the fundamental gap in the $\{211\}\Sigma = 3$ boundary and in the $\{130\}\Sigma = 5$ boundary in Si. In these calculations, we have found some boundary localised states at the band edges. But these states are buried under the bulk band edges of the density of states and do not contribute to band tails. It seems that the electrical activity of grain boundaries is associated with irregularities such as defects induced in the CSL boundaries or irregular boundaries [1, 4, 5].

Bourret and Bacmann [6, 7], using HREM, have already observed several types of defects in the $\langle 011 \rangle$ symmetrical tilt grain boundaries in Ge. These defects are secondary dislocations, steps, facets and grain boundary dissociations. They have developed atomic models of these defects from the HREM images. Similar defects have also been observed in Si [14–16]. Nowadays, it is essential to study the structural and electronic properties of these defects in the CSL boundaries as well as the effects of segregation or precipitation of impurities at grain boundaries.

In this Letter, we have calculated the atomic and electronic structure of the $\{211\}/\{111\}$ facets as defects in the CSL boundaries in Si. The $\Sigma = 3$ first-order twin boundaries often show facetting on $\{111\}$ and $\{211\}$ planes in polycrystalline Si and Ge [1, 6, 7, 16]. Otherwise, $\{111\}$ steps perpendicular to the $\{211\}$ plane frequently appear

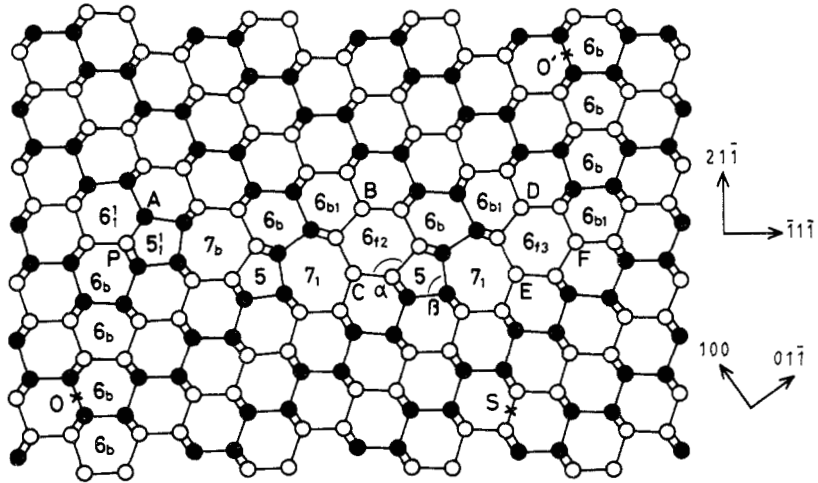


Figure 1. [011] projection of the atomic model of the $\{211\}/\{111\}$ facets in Si. Atoms represented by open and closed circles are displaced from each other by about $\sqrt{2}a_{0/4}$ along the [011] direction. One more set of atoms is included in one period along the [011] axis. The structural units at the interface are indicated by the symbols proposed by Papon and Petit [18]. Atoms indicated by A, B, C, D, E and F constitute the reconstructed bonds along the [011] direction. The points O and O' indicate one period of the $\{211\}/\{111\}$ facets and the point S is a symmetric point in the present supercell geometry.

in the $\{211\}\Sigma = 3$ twin. There have been several experiments indicating that the electrical activity is associated with these types of facets or steps [1, 17]. Bourret and Bacmann [6, 7] have observed a coherent $\{111\}$ step in the $\{211\}\Sigma = 3$ twin boundary in Ge by using HREM and have developed an atomic model. We have constructed an atomic model of the $\{211\}/\{111\}$ microfacets in Si from their model, as shown in figure 1. The structural units at the interfaces are indicated by the symbols proposed by Papon and Petit [18]. It is interesting that complete reconstruction is also possible at the junctions of the $\{111\}$ and $\{211\}$ planes by introducing reconstruction schemes along the [011] axis as well as in the $\{211\}$ interfaces. There are two types of the facet junctions and new structural units exist at the junctions. One of these two types of junctions contains (at A in figure 1) a particular reconstruction scheme, the $D_1 + S$ reconstruction [7], which introduces a large shear around itself. The other junction (at F in figure 1) contains an ordinary reconstruction scheme, the D_1 reconstruction, as does the $\{211\}$ segment.

In this model, the $\{111\}$ interfaces are introduced at the location of the 6_b and 5 units in the $\{211\}$ interface. This is because the atomic heights along the [011] direction coincide with each other at the $\{111\}$ interface introduced at this location, and because the size of each of the two atomic rings, the 6_b and 5 units, along the $[2\bar{1}\bar{1}]$ direction is suitable for the replaced two six-membered rings at the facet junctions. The atomic structures at the facet junctions in figure 1 are compatible with the $\{211\}$ and $\{111\}$ segments of other sizes. The present model of the facet junctions can be regarded as a general one. It is important to examine the structural and electronic properties of the regions of the facet junctions because the properties of the $\{211\}$ and $\{111\}$ segments themselves have already been examined [10, 11, 13].

We have used a supercell technique for calculations of the electronic structure. In the present supercell geometry shown in figure 1, periodicity from O to O' is imposed

along the direction of \mathbf{OO}' . Therefore, the $\{211\}$ segments of length about 1.9 nm and the $\{111\}$ segments of length about 2.0 nm are repeated alternately. The periodicity along the $[011]$ axis is twice as long as that in the perfect crystal because of reconstruction along the $[011]$ axis. Another periodicity is also imposed by arranging other faceted twin boundaries with inversion symmetry alternately. The symmetric point is indicated by S in figure 1. In this way, each unit cell contains 704 atoms. The $\{211\}$ segment of the present model contains one-and-a-half periods of the (2×2) cm structure [7]. Of course, the present supercell geometry has been selected by the restriction of computing power. The effects of the sizes of the respective segments of the facets and the distance between the neighbouring symmetric faceted twins in the supercell geometry are important, especially in connection with the elastic distortions induced by the different rigid-body translations of the $\{211\}$ and $\{111\}$ interfaces; this problem should be investigated in the future. The main purpose of the present study is to examine the local atomic and electronic structures of the disordered regions at the facet junctions.

Because of the large number of the atoms in the supercell, it is not easy to perform energy-minimisation calculations via calculations of electronic structure as in previous works [12, 13]. Thus, the optimum atomic structure in the supercell geometry was determined by energy-minimisation calculations in the Keating model [19]. The optimum rigid-body translation between the two crystals constituting the faceted twin was also determined. Figure 1 shows this optimum structure. The rigid body translation along the $[\bar{1}\bar{1}\bar{1}]$ direction inherent in the $\{211\} \Sigma = 3$ twin boundary moves the upper crystal toward the right-hand side against the lower crystal in figure 1, but the presence of the $\{111\}$ steps decreases this translation. Thus the compressive stress is induced for the $\{111\}$ interfaces. In figure 1, the translation along the $[\bar{1}\bar{1}\bar{1}]$ direction is more visible in the arrays of atomic columns in the central region of the $\{211\}$ segment as compared with the neighbourhood of the $\{111\}$ steps. This can be also found in the HREM image in Ge in [6]. The atomic structure of the boundary core in the central region of the $\{211\}$ facet is not so different from that of the straight $\{211\} \Sigma = 3$ boundary in our previous calculation [13]. For example, the bond length deviations of the reconstructed bonds along the $[011]$ axis at B and C in figure 1 are +2.07% and +2.42%, respectively, and the bond angle deviations at α and β in figure 1 are +15.0° and -21.0°, respectively. These are +2.46%, +2.42%, +17.5° and -18.8° in the straight twin boundary.

As for the regions of the facet junctions, relatively large distortions exist, especially at one of the two types of junctions. Figure 2 shows the $[\bar{1}\bar{1}\bar{1}]$ projections of the atomic positions and the calculated local distortion energies of atoms of the $D_1 + S$ reconstruction at A and of the D_1 reconstruction at F in figure 1. As shown in figure 2(b), local distortion energies around the D_1 reconstruction are in the same range as those in the region of the $\{211\}$ segment. Thus it can be said that reconstruction can occur easily at this type of the facet junction as well as in the $\{211\} \Sigma = 3$ twin boundary. On the other hand, as shown in figure 2(a), relatively large distortion energies exist around the $D_1 + S$ reconstruction because this type of reconstruction requires a shear along the $[011]$ axis. The deviations in bond lengths in this region are in the same range as those in the other regions, but the deviations in bond angles are relatively large in this region. Particularly, the bond angle deviations around the atom indicated by P in figures 1 and 2(a) range from -33.1° to +25.4° and the energy of this atom is high.

Buis and co-workers [1] have found that a high density of microfacets or dislocations is introduced at only one side of the facet junctions in the $\{211\}/\{111\}$ facets of the order of μm . This observation is probably connected with the present atomic model where high distortion energy must be introduced at only one side of the facet junctions. When

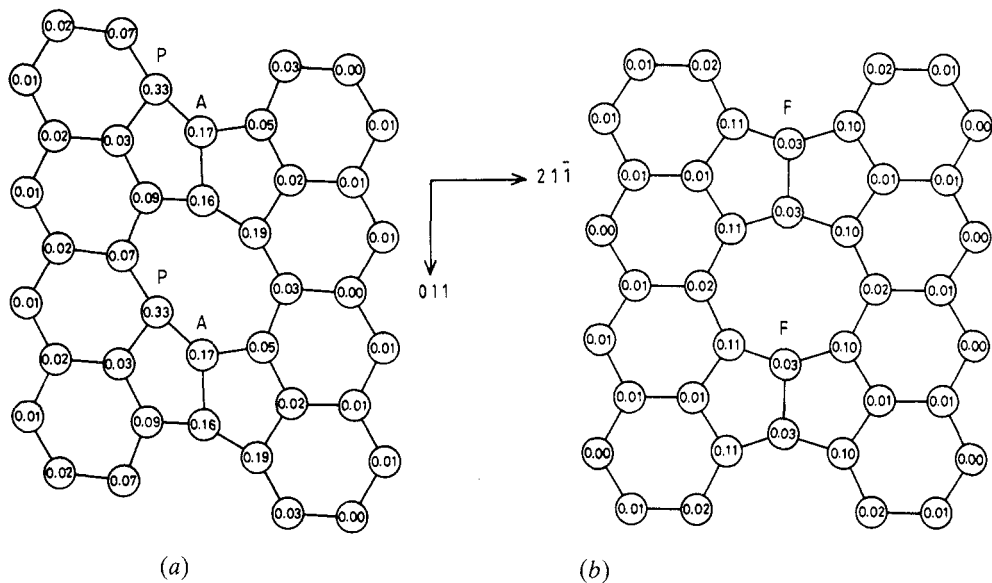


Figure 2. (a) Side view of the reconstruction at A in figure 1 and local distortion energies of atoms. The energies are expressed in eV. (b) Side view of the reconstruction at F in figure 1 and local distortion energies of atoms.

the lengths of the $\{211\}$ and $\{111\}$ segments are large enough, the elastic stress in the vicinities of the facet junctions caused by the different rigid body translations of the two interfaces is considered to be fairly high as compared with the facets with segments of short lengths. It seems that the problems of the elastic stress caused by the different rigid body translations at the interfaces and of the microscopic atomic structure of the facet junctions are important in deciding the stability and the shape of the $\{211\}/\{111\}$ facets, which should be investigated in future.

The electronic structure of the present optimum geometry in figure 1 has been calculated using a first-neighbour tight-binding model with parameters given in [20], which provide a reasonable description of the electronic structure of bulk Si. These parameters were assumed to have a d^{-2} dependence on the nearest-neighbour distance d . From the supercell method, in contrast to the recursion method [10, 11], one can obtain more detailed information in k -space about electronic structure [12, 13]. In the present supercell geometry, the two-dimensional periodicity parallel to the (011) atomic plane, that is the xz plane in the present notation, is fairly large as compared with the period along the [011] axis. Thus, the quasi-one-dimensional band structure along the [011] direction has been calculated by diagonalisation of 2816×2816 Hamiltonian matrix for several k -points with $k_x = k_z = 0$.

The results are shown in figure 3. There are no deep states in the fundamental gap, in accordance with the absence of dangling bonds. At least, the atomic structure of the $\{211\}/\{111\}$ facets deduced from the HREM image by Bourret and Bacmann [6, 7] does not cause deep levels in Si. However, there exists a doubly degenerate band inside the gap indicated by an arrow in figure 3, although these states are above the bulk conduction-band minimum. This shallow band seems to be different from the boundary localised states at the band edge in the $\{211\}$ $\Sigma = 3$ twin boundary found in our previous calculation [13]. By the analysis of the eigenvectors, some states of this band are found to

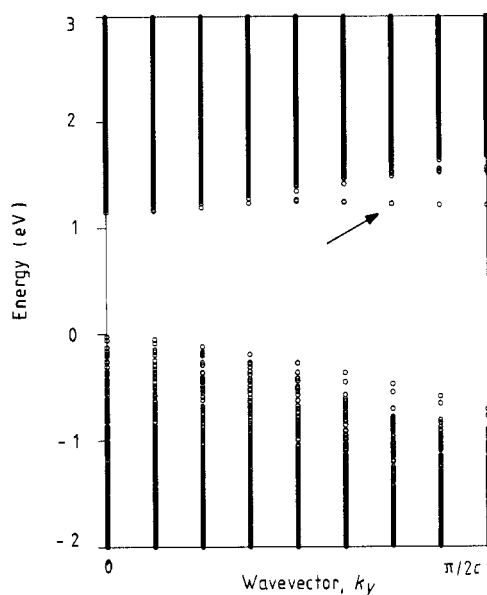


Figure 3. Energy band structure along the [011] direction of the atomic model of the $\{211\}/\{111\}$ facets in Si shown in figure 1. Calculated eigenstates of the 704-atom unit cell are represented. c is $\sqrt{2}a_1/2$. An arrow indicates a band considered to be connected with the reconstruction at A in figure 1.

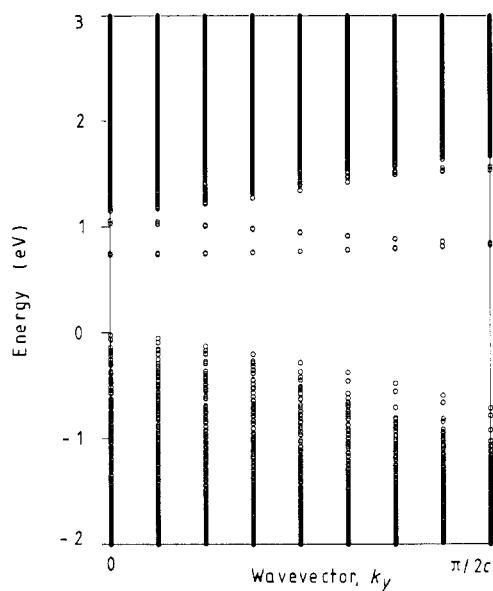


Figure 4. Energy band structure of the atomic model with the reconstruction at A in figure 1 replaced by dangling bonds. Two dangling bond bands appear in the fundamental gap.

be localised in the vicinity of the facet junction including the $D_1 + S$ reconstruction. However, other states in this band are not found to be localised clearly by this analysis.

In order to elucidate the origin of this shallow band more clearly, we have calculated the electronic structure of the atomic model where the $D_1 + S$ reconstruction at A in figure 1 is replaced by dangling bonds. This structure has been relaxed using the same Keating-type potential [19] and large distortions around the $D_1 + S$ reconstruction are removed. The results are shown in figure 4. Two doubly degenerate dangling bond bands appear in the fundamental gap in figure 4. This corresponds with there being two sets of two types of dangling bonds in one supercell. But the band indicated by an arrow in figure 3 does not exist in figure 4. Thus, it is clear that this band is connected with localised distortions caused by the $D_1 + S$ reconstruction at the facet junction.

It should be noted that states other than those connected with the $D_1 + S$ reconstruction are not so different from each other in figure 3 and figure 4. By comparing the electronic states at the band edges with the projected states of the perfect crystal, localised states exist at the conduction-band-edge similar to those found in our previous calculation of the $\{211\}$ interface [13]. These states should be caused by the disordered regions other than the $D_1 + S$ reconstruction.

In this way, it is clear that the disordered region including the $D_1 + S$ reconstruction at the facet junction perturbs the electronic structure much more than the $\{211\}$ and the $\{111\}$ interfaces. However, it should be noted that the shallow band caused by this region exists above the bulk conduction-band minimum and does not lie inside the minimum gap in figure 3. Of course, we do not deny the possibility that the energy levels of this

band might be changed in calculations by more reliable theoretical schemes than the present tight-binding model, and this band might be connected with band tails observed in polycrystalline semiconductors. However, the present results agree with the prediction that only very strongly distorted bonds can induce localised states inside the fundamental gap in Si [21].

Of course, there is a possibility that the structure with dangling bonds instead of the $D_1 + S$ reconstruction is more stable. The decrease in calculated elastic energy by replacing the $D_1 + S$ reconstruction with two dangling bonds is 0.68 eV in the present Keating model. As compared with the discussion about the reconstruction in the core structure of dislocations [22], it seems that the $D_1 + S$ reconstruction could exist stably, although it is unable to deal correctly with the effect of rehybridisation in atoms with dangling bonds and the energy of a dangling bond in the Keating model. In any case, the electronic structure is considerably perturbed by the disordered structure of the facet junctions as compared with the $\{211\}$ and $\{111\}$ interaces.

In summary, relatively large distortions exist at one of the two types of facet junctions in the $\{211\}/\{111\}$ facets. This region perturbs the electronic structure much more than the $\{211\}$ and the $\{111\}$ interfaces, but introduces no states inside the minimum gap. Therefore, on condition that the present atomic structures of the facet junctions exist stably, the origin of the observed electrical activity of the microfacets or steps [1, 17] should be attributed to extrinsic effects, such as antiphase defects [23] impurity segregation or precipitation at highly distorted regions at the facet junctions.

References

- [1] Buis A, Oei Y-S and Schapink F W 1986 *Trans. Japan Inst. Met., Suppl.* **27** 221
- [2] Stützer F J, Madenach A J, Werner J, Lu Y C and Queisser H J 1986 *Trans. Japan Inst. Met., Suppl.* **27** 1005
- [3] Poullain G, Bary A, Mercey B, Lay P, Chermant J L and Nouet G 1986 *Trans. Japan Inst. Met., Suppl.* **27** 1069
- [4] Yasutake K, Takeuchi A, Tanaka Y, Yoshii K and Kawabe H 1987 *Technical Digest Int. PVSEC-3, Tokyo* p 409
- [5] Shimokawa R and Hayashi Y 1988 *Japan J. Appl. Phys.* **27** 751
- [6] Bourret A and Bacmann J J 1985 *Surf. Sci.* **162** 495
- [7] Bourret A and Bacmann J J 1986 *Trans. Japn Inst. Met., Suppl.* **27** 125
- [8] Thomson R E and Chadi D J 1984 *Phys. Rev. B* **29** 889
- [9] DiVincenzo D P, Alerhand O L, Schlüter M and Wilkins J W 1986 *Phys. Rev. Lett.* **56** 1925
- [10] Mauger A, Bourboin J C, Allan G, Lannoo M, Bourret A and Billard L 1987 *Phys. Rev. B* **35** 1267
- [11] Paxton A T and Sutton A P 1988 *J. Phys. C: Solid State Phys.* **21** L481
- [12] Kohyama M, Yamamoto R, Ebata Y and Kinoshita M 1988 *J. Phys. C: Solid State Phys.* **21** 3205
- [13] Kohyama M, Yamamoto R, Watanabe Y, Ebata Y and Kinoshita M 1988 *J. Phys. C: Solid State Phys.* **21** L695
- [14] Ichinose H, Tajima Y and Ishida Y 1986 *Trans. Japan Inst. Met., Suppl.* **27** 253
- [15] Elkajbaji M and Thibault-Desseaux J 1988 *Phil. Mag. A* **58** 325
- [16] Garg A, Clark W A T and Hirth J P 1989 *Phil. Mag. A* **59** 479
- [17] Sharko R, Gervais A and Texier-Hervo C 1982 *J. Physique Coll.* **43** C1 129
- [18] Papon A M and Petit M 1985 *Scr. Metall.* **19** 391
- [19] Baraff G A, Kane E O and Schlüter M 1980 *Phys. Rev. B* **21** 5662
- [20] Chadi D J 1984 *Phys. Rev. B* **29** 785
- [21] Petit J, Lannoo M and Allan G 1987 *Phys. Rev. B* **35** 2863
- [22] Marklund S 1980 *Phys. Status Solidi b* **100** 77
- [23] Heggie M and Jones R 1983 *Phil. Mag. B* **48** 365